ELSEVIER

Wear 242 (2000) 18–27

WEAR

www.elsevier.com/locate/wear

Friction and wear behavior of Ti following laser surface alloying with Si, Al and Si + Al

J. Dutta Majumdar [a], B.L. Mordike [b], I. Manna [a,*]

[a] *Metallurgical and Materials Engineering Department, Indian Institute of Technology, Kharagpur 721302, India*
[b] *Institüt für Werkstoffkunde und Werkstofftechnik, TU Clausthal, Agricolastraße 6, D-38678 Clausthal–Zellerfeld, Germany*

Received 19 May 1999; received in revised form 29 February 2000; accepted 29 February 2000

Abstract

This study concerns the friction and wear behavior of Ti following laser surface alloying (LSA) with Si, Al or Si + Al. The said tribological characteristics of the laser-alloyed samples, subjected to the earlier determined optimum conditions of LSA, were investigated in terms of the variation of wear depth as a function of load and time using a computer-controlled reciprocating ball-on-disc wear testing machine fitted with an oscillating hardened steel ball. A detailed post wear microstructural analysis was conducted to determine the mechanism of wear and role of alloying elements in improving the resistance to wear. It appears that LSA with Si is more effective in improving the wear resistance of Ti than that by Si + Al or Al alone. The enhanced wear resistance in Si surface alloyed samples has been attributed to the presence of uniformly distributed Ti_5Si_3 in the alloyed zone (AZ).

Keywords: Laser surface alloying; Wear resistance; Friction; Titanium; Silicon; Aluminum

1. Introduction

Ti and its alloys are extensively used in jet engine compressor components, high-pressure heat exchangers, sea water desalination plants, offshore structures and petrochemical plants owing to their high specific mechanical strength and corrosion resistance [1]. However, the wear resistance of Ti/Ti alloys is inadequate in many of these applications. It is known that the microstructural changes obtained by heat-treating Ti alloys may impart marginal improvement in the sliding wear resistance [2]. Miller and Holladay [3] have reported that wear resistance could be partially improved through surface modification provided the adhesion of the coating to the substrate is strong. In this regard, Beck and Danovich [4] have experimentally examined the usefulness of stronger coating–substrate bonding in the case of diffusion bonded electroless Ni coating on Ti alloys. Similar strong coating–substrate bonding is possible in the glow discharge ion-nitriding process [5,6]. Though such nitrided layer is characterized by high hardness, the thickness of the said layer is usually very low (2–3 μm).

In the recent past, several attempts have been made to improve the wear resistance of Ti alloys by laser surface alloying (LSA) [7–10]. LSA involves rapid melting, intermixing and solidification of the pre- or co-deposited alloying elements with a part of the underlying substrate to form an alloyed zone (AZ) confined only to the near-surface region within a very short interaction time [11–13]. The process is characterized by an extremely high heating/cooling rate (10^4 to 10^{10} K/s), thermal gradient (10^5 to 10^8 K/m) and solidification velocity (maximum of up to 30 m/s) [12]. As a consequence, LSA may extend the solid solubility limit, and result in a metastable and novel microstructure. Mordike [14] has suggested that laser assisted gas nitriding could significantly enhance the hardness in pure Ti or Ti–6Al–4V. Ayers [15] has attempted a similar improvement by injecting carbide particles during laser surface melting of Ti/Al-alloys. Subsequently, Yarramarreddy and Bahadur [16] have studied the tribological behavior of Ti–6Al–4V subjected to laser surface melting and LSA.

* Corresponding author. Tel.: +91-3222-83266; fax: +91-3222-55303.
E-mail address: imanna@metal.iitkgp.ernet.in (I. Manna).

0043-1648/00/$ - see front matter
PII: S0043-1648(00)00363-X

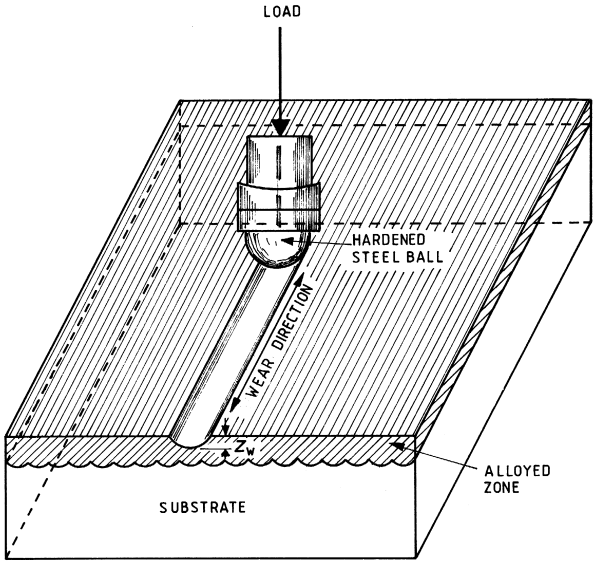

Fig. 1. Schematic diagram of the reciprocating ball-on-disc wear testing set up.

Recently, the present authors have achieved a significant improvement in the high-temperature oxidation resistance of Ti (both under isothermal and cyclic conditions) by LSA with Si and Si + Al [17–19]. In the present study, the scope and extent of improving the tribological properties (hardness, friction and wear) of pure Ti following LSA with Si, Al or Si + Al have extensively been studied. In addition, the mechanism and different stages of wear of the laser-alloyed samples have been identified in terms of the variation of coefficient of friction with time.

2. Experimental method

Prior to LSA, pure Ti specimens were subjected to sand blasting to clean the surface and improve absorptivity. LSA was carried out by a 6 kW continuous wave CO_2 laser with a rectangular beam of 3.45×2.4 mm^2 area (with the focal point resting 35 mm above the surface) by co-deposition or simultaneous feeding of Si (22–45 μm size), Al (64–100 μm size) or a mixture of Si + Al (Si:Al (by weight) = 3:1) powders through an Ar gas driven (6 l/min) powder delivery system. The elemental powders used for alloying were of more than 99.5% purity. Henceforth, the Si, Al and Si + Al surface-alloyed specimens (on Ti) would be called Ti(Si), Ti(Al) and Ti(Si + Al), respectively. LSA was carried out with the following range of process parameters [18]: incident laser power (P = 2 to 4.5 kW), linear scanning speed of the specimen stage (v = 200 to 550 mm/min) and powder feed rate (F_P = 16 to 80 mg/s). Following LSA, the microstructure of the AZ was characterized using a scanning electron microscope (SEM). Compositional analysis of the AZ was carried out by the energy dispersive spectroscopy (EDS) along with SEM analysis. Subsequently, the constituent phases in the AZ prior to wear studies were identified through a careful X-ray diffraction (XRD) analysis using a CuK_α (wavelength, $\lambda = 0.154$ nm) radiation.

Variation of microhardness (H_v) was determined on a plane perpendicular to both the top/lased surface and lasing direction (henceforth, to be called the cross-sectional plane) as a function of the vertical depth from the surface (z) by a Vickers microhardness tester. The friction and wear behavior of the specimens (as-received and laser-alloyed) were studied by a reciprocating ball-on-disc wear testing machine. The wear test included multiple wearing of the specimen surface with the help of a reciprocating hardened steel ball (100Cr6) of 5 mm diameter with varying loads (L) from 10 to 60 N. Fig. 1 schematically illustrates the reciprocating ball-on-disc wear test set-up. The respective wear period, wear speed and wear length were maintained constant at 4 s, 50 mm/min and 3.3 mm, respectively, throughout the study. The multipass wear tracks consisted of 10 to 1000 number of wear cycles (n_w), each comprising a 3.3 mm long forward and reverse operation. The tangential force (L_t) was recorded (directly from the computer-controlled output of the profilometer) as a function of n_w at different L to evaluate the possible adhesive force at the interface between the steel balls and specimen surfaces. Subsequently, the depth of wear (z_w) was determined by measuring the maximum surface roughness index (R_{max}) produced due to wear by a profilometer. Here, the use of a profilometer to measure z_w was necessary because z_w was often too low to measure by cross-sectional optical microscopy. The effects of n_w and L on z_w were analyzed. The kinetics of material loss were determined by plotting z_w as a function of n_w or total time of wear (t_w). Similarly, the variation of L_t as a function of n_w and L was investigated to assess the coefficient of friction (μ) under different conditions. Finally, the worn-out surfaces were examined under the

Table 1
Optimum processing conditions (P, v and F_p) for LSA of Ti with Si, Al and Si + Al and the corresponding properties (w, R_{max}, X_{Si}, X_{Al} and H_v) of the AZ

System	Optimum parameters			Properties of the AZ				
	P (kW)	v (mm/min)	F_p (mg/s)	w (mm)	R_{max} (μm)	X_{Si} (at.%)	X_{Al} (at.%)	H_v (VHN)
Ti(Si)	3–4.2	175–450	16–20	0.6–1.2	25–29	11–16	–	700–750
Ti(Al)	2.9–4.25	175–550	16–20	0.7–1.5	19–21	–	12–14	400–450
Ti(Si + Al)	3–4.2	200–400	16–20	0.5–1.0	24–27	7–9.5	2–4	575–650

SEM in the secondary electron mode to find out the mechanism of wear in laser-alloyed samples.

3. Results and discussions

3.1. Laser processing

The final microstructure, composition and properties following LSA of a given system are strongly dependent on the process parameters employed (P, v and F_p) [17–19]. Table 1 summarizes the optimum LSA parameters selected in this study to obtain the desired microstructure, composition, microhardness and surface roughness. It may be mentioned that the process of optimizing the LSA routines involved an elaborate scheme of investigations with suitable evaluation at the appropriate stages [18].

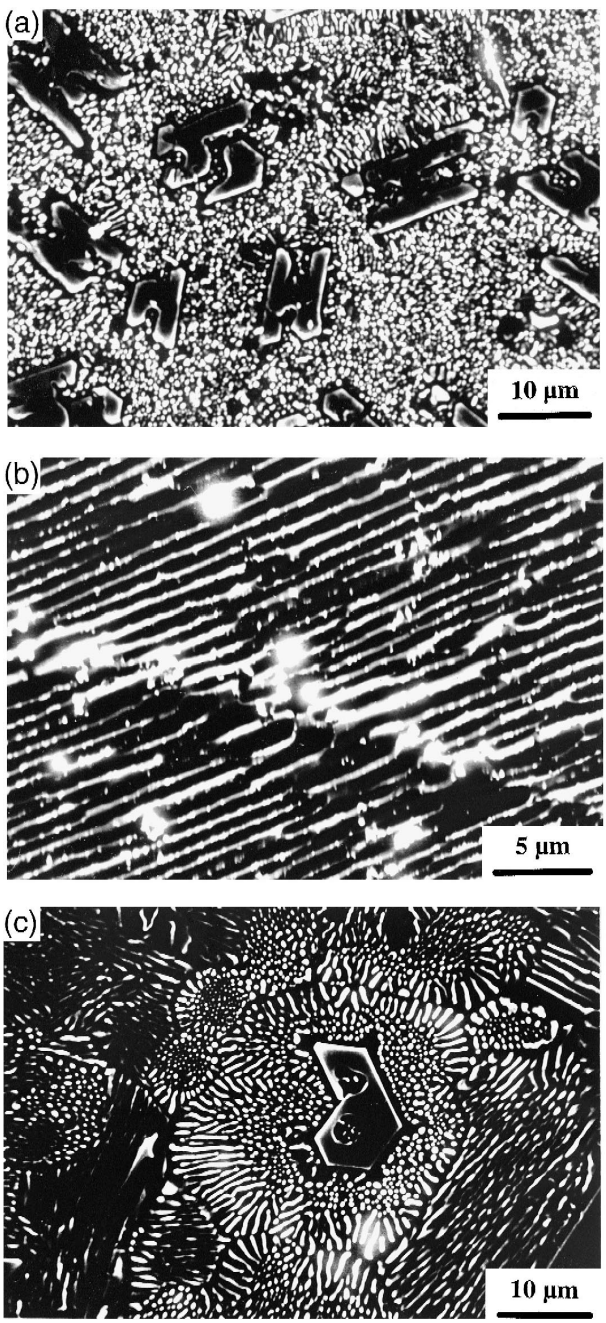

Fig. 2. Microstructure of the top surface of laser-alloyed Ti with (a) Si, (b) Al and (c) Si + Al. Note that (a) and (c) show hyper-eutectic and (b) reveals single phase lamellar microstructures. LSA was carried out with $P = 4$ kW, $v = 300$ mm/min and $F_p = 16$ mg/s.

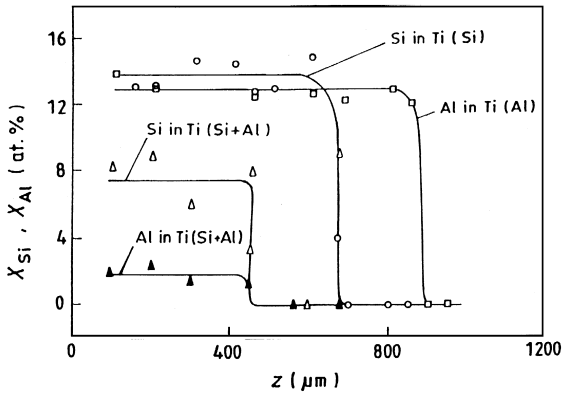

Fig. 3. Variation of the solute contents (X_{Si} or X_{Al}) in the AZ as a function of depth (z) from the surface. LSA was carried out with $P = 3.5$ kW, $v = 300$ mm/min and $F_p = 17$ mg/s.

3.2. Microstructure

Fig. 2(a)–(c) show the representative microstructures of the top surfaces of the AZ (lased with $P = 3.5$ kW, $v = 300$ mm/min and $F_p = 16$ mg/s) of Ti(Si), Ti(Al) and Ti(Si + Al), respectively. Fig. 2(a) reveals a typical hyper-eutectic microstructure comprising the faceted Ti_5Si_3 phases uniformly distributed in the two-phase eutectic aggregate of α-Ti and Ti_5Si_3. The high volume fraction of the primary phase signifies complete dissolution and uniform intermixing of Si. Similarly, the degree of fineness of the eutectic products is due to the rapid quenching experienced by the AZ. Furthermore, the greater volume fraction of the primary phase (say, in Fig. 2(a)) than that expected in the equilibrium microstructure of an alloy with 11–16 at.% Si (i.e., the average solute content in Ti(Si); Table 1) may be attributed to the effect of non-equilibrium solidification induced by LSA under the present routines on the resultant microstructure. On the other hand, the AZ of Ti(Al) is characterized by a single phase microstructure comprising the quenched-in parallel α-Ti lamellae or α′ martensite plates (Fig. 2(b)). Al stabilizes the α-phase in Ti [20]. Thus, it is anticipated that rapid quenching in the present LSA routine has precluded phase separation during solidification and retained a single phase microstructure of α-Ti(Al). In Ti(Si + Al), the microstructure reveals a typical hyper-eutectic structure with uniform distribution of primary Ti_5Si_3 in the eutectic matrix of α-Ti + Ti_5Si_3 (Fig. 2(c)) as that in Ti(Si) (Fig. 2(a)). However, Fig. 2(c) differs from Fig. 2(a) only in terms of the volume fraction

of the primary phase and degree of fineness of the eutectic aggregate.

3.3. Composition and phase analysis

Fig. 3 displays the variation of the concentration of the alloying elements in terms of total Si content (X_{Si}) and total Al content (X_{Al}) determined by EDS analysis with z along the cross-sectional plane of Ti(Si), Ti(Al) and Ti(Si + Al) (processed with $P = 3.5$ kW, $v = 300$ mm/min and $F_p = 17$ mg/s), respectively. It is evident that the solute concentration in all the specimens is almost uniform within the AZ and drops sharply to zero as z exceeds the AZ depth (w). The occasional scatter of X_{Si} about the mean composition (say, in Ti(Si + Al)) may be attributed to the presence of a primary phase dispersed in the eutectic aggregate in the concerned microstructure.

Fig. 4(a)–(c) present the respective XRD profile obtained from the top surface of laser-alloyed Ti(Si), Ti(Al) and Ti(Si + Al) (lased with $P = 3.5$ kW, $v = 300$ mm/min and $F_p = 17$ mg/s). It may be noted that only α-Ti and Ti_5Si_3 peaks are present in Ti(Si). The XRD pattern of Ti(Si + Al) reveals similar peaks of α-Ti and Ti_5Si_3 with a systematic shift of the α-Ti peak positions. On the other hand, the XRD pattern of Ti(Al) is characterized only by the α-Ti peaks with an identical systematic shift in the

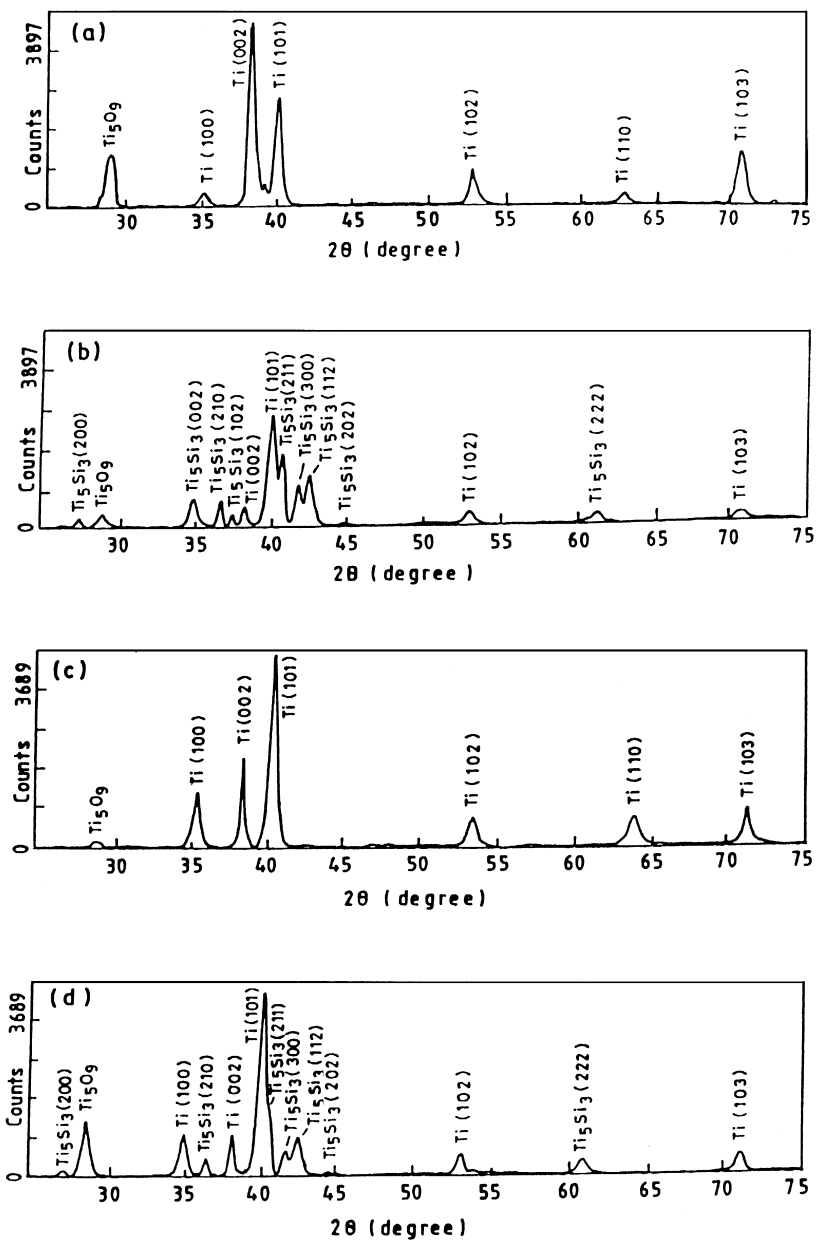

Fig. 4. XRD profiles of the top surface of (a) pure Ti, and that of laser-alloyed Ti with (b) Si, (c) Al and (d) Si + Al. LSA was carried out with $P = 3.5$ kW, $v = 300$ mm/min and $F_p = 17$ mg/s.

respective peak positions. The average Al content in the AZ in solid solution with Ti was determined from the relevant data on solid solubility of Al in Ti available in the literature [21].

3.4. Microhardness

Fig. 5 shows the variation of H_v in the AZ as a function of z. It is apparent that LSA has resulted in a significant improvement (two to four times) in the average H_v level in the AZ as compared to that in the substrate region. In Ti(Al), the H_v level remains nearly constant throughout the AZ. In contrast, the H_v distribution in the AZ of Ti(Si) is non-uniform and shows a random scatter about a mean value as a function of z. This difference in the H_v profiles may be related to the single phase and hyper-eutectic microstructure in Ti(Al) vis á vis Ti(Si)/Ti(Si + Al), respectively (Fig. 2). Thus, the H_v distribution in the AZ substantiates the earlier results on the microstructure and composition in the AZ of the respective specimens. Finally, it may be pointed out that Si seems more effective in raising the H_v level in the AZ than that by Al due to the presence of the hard Ti_5Si_3 (both as primary and a eutectic constituent) phases in the Ti(Si) and Ti(Si + Al) surfaces. A careful comparison between Figs. 3 and 5 reveals that z up to which H_v and X_{Si} or X_{Al} levels are significantly higher than those of the substrate (i.e., Ti) are identical and equal to the corresponding values of w determined earlier from the microstructure on the cross-sectional plane [18]. Thus, it is evident that LSA is primarily responsible for the increase in H_v in the AZ.

3.5. Wear resistance

The variation of z_w with L of pure Ti, Ti(Si), Ti(Al) and Ti(Si + Al) following wear by a hardened steel ball is presented in Fig. 6. It may be noted that z_w varies linearly

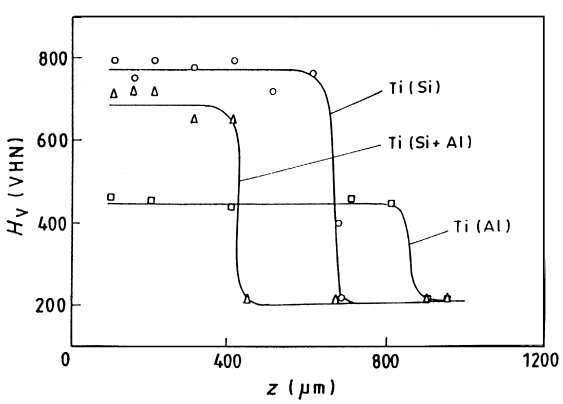

Fig. 5. Variation of H_v in the AZ of Ti(Si), Ti(Al) and Ti(Si + Al) as a function of z. LSA was carried out with $P = 3.5$ kW, $v = 300$ mm/min and $F_p = 17$ mg/s.

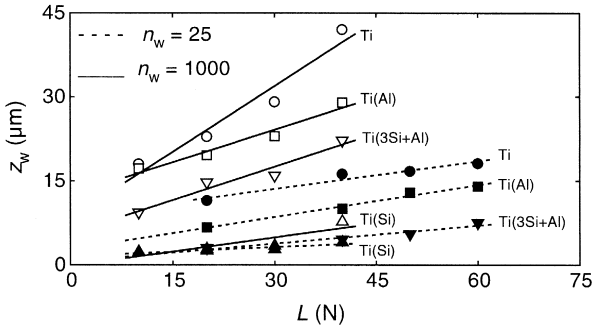

Fig. 6. Variation of depth of wear (z_w) with load (L) of pure Ti and laser-alloyed Ti with Si, Al and Si + Al lased with $P = 4$ kW, $v = 300$ mm/min and $F_p = 17$ mg/s. The continuous lines with open symbols and broken lines with filled symbols represent the data for $n_w = 1000$ and 25, respectively.

with L in all the cases. The effect of L on z_w is more prominent at higher n_w (= 1000) than that at a lower value of the same (= 25). Under comparable conditions of wear, Ti undergoes the most rapid wear loss followed by that in Ti(Al), Ti(Si + Al) and Ti(Si). Ti(Si) undergoes the minimum wear loss. According to the equation of Archard [22], the volume of wear loss (Y) under constant L is:

$$Y = kLut_w/H_v, \quad (1)$$

where, u is the sliding speed and k is a constant usually referred to as the wear coefficient. Hence, the volume of wear loss is proportional to L and inversely proportional to H_v for a given t_w and u.

It has already been shown that LSA increases the H_v level of pure Ti by two to four times (Fig. 5). Furthermore, the effect is most significant in Ti(Si) followed by that in Ti(Si + Al) and Ti(Al) in order of decreasing H_v. Thus, it is quite logical to anticipate (according to Eq. (1)) that the wear loss would be minimum in Ti(Si) followed by that in Ti(Si + Al) and Ti(Al) under comparable conditions of wear, which is indeed true in the present investigation (Fig. 6).

Fig. 7 shows the variation of z_w with n_w (or t_w) due to wear at two different L. The extent and rate of wear

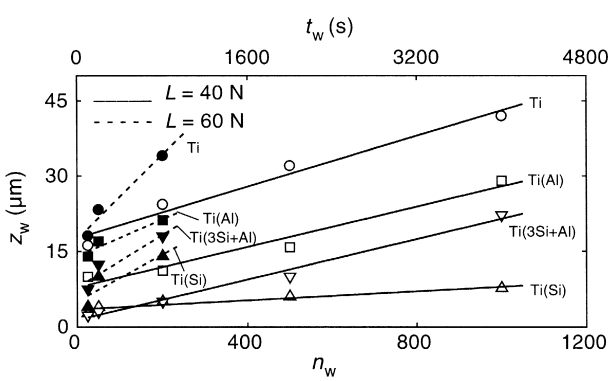

Fig. 7. Variation of depth of wear (z_w) with the number of cycles (n_w) and time of wear (t_w) of pure Ti and laser-alloyed Ti with Si, Al and Si + Al lased with $P = 4$ kW, $v = 300$ mm/min and $F_p = 17$ mg/s.

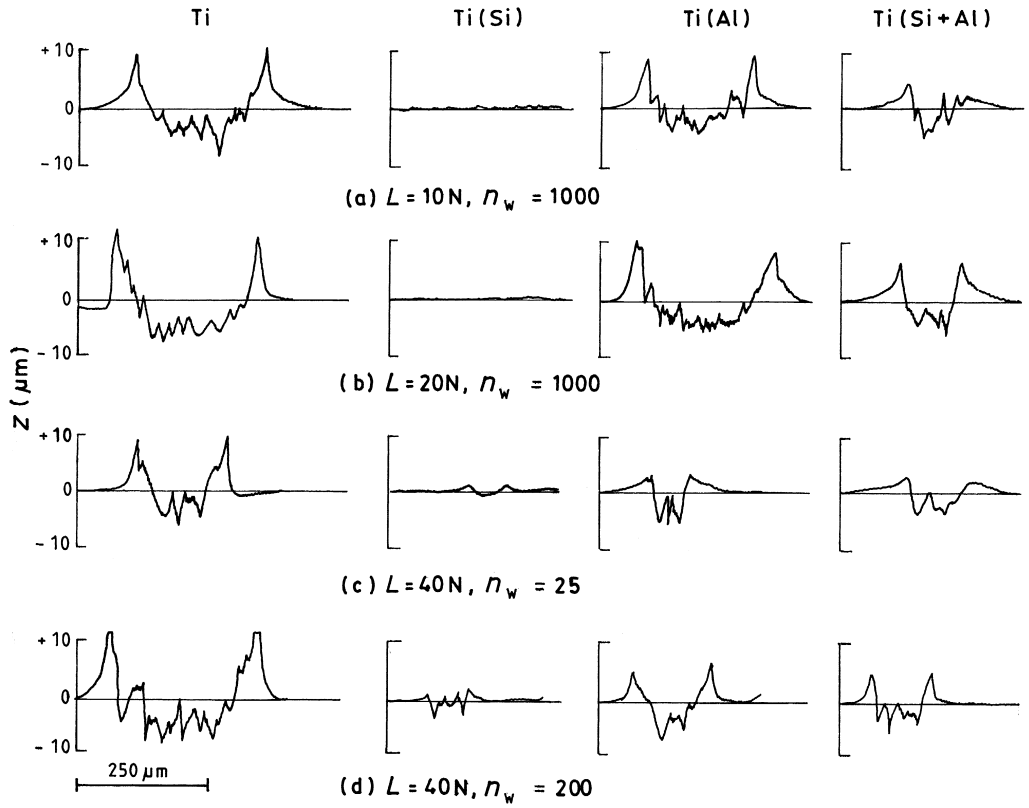

Fig. 8. Variation of size/depth and shape of wear tracks for different conditions of wear testing with a hardened steel ball in terms of L and n_w in (a) Ti, and laser-alloyed Ti with (b) Si, (c) Al and (d) Si + Al. Note that wear depth increases with an increase in L or n_w under comparable conditions, and the damage, in general, is minimum in Ti(Si).

increase with an increase in n_w (or t_w), especially at higher L. Comparison of the wear depth and slopes of the plots suggest that the rate of wear loss is maximum in Ti and minimum in Ti(Si). It may be pointed out that the bulk of the respective sets of results presented in Fig. 7 are in perfect agreement with Eq. (1).

Fig. 8(a)–(d) show the variation in size/depth and shape of the worn-out tracks made by the oscillating hardened steel ball with different wear parameters in pure Ti, Ti(Si), Ti(Al) and Ti(Si + Al), respectively. It is immediately apparent that the wear loss is minimum in Ti(Si) followed by that in Ti(Si + Al), Ti(Al) and pure Ti (in increasing order) under comparable conditions. A careful comparison reveals that both the width and depth of wear increase independently with an increase in L or n_w for a given material under identical conditions. In Ti(Si), any noticeable wear with $L = 20$ N is absent even after $n_w = 1000$. A measurable wear in Ti(Si) initiates only at $L = 40$ N after $n_w > 25$. Thus, it is evident that LSA of Ti with Si, Si + Al and Al significantly improves the resistance to wear than that in pure Ti.

3.6. Coefficient of friction (μ)

The coefficient of friction (μ) is expressed as:

$$\mu = L_t/L. \quad (2)$$

Fig. 9(a) and (b) illustrate the effect of L on μ due to wear with a hardened steel ball for $n_w = 1000$ and 25, respectively. At a higher n_w ($= 1000$), μ decreases or

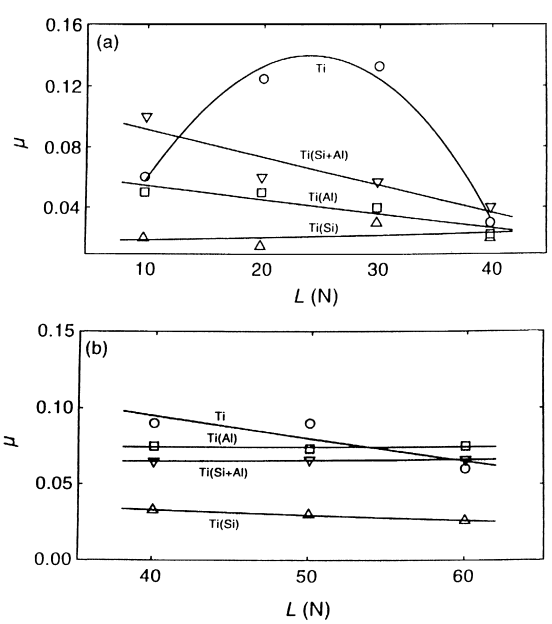

Fig. 9. Effect of L on μ in pure Ti, Ti(Si), Ti(Al) and Ti(Si + Al) with (a) $n_w = 1000$, and (b) $n_w = 25$. LSA was carried out with $P = 4$ kW, $v = 300$ mm/min and $F_p = 17$ mg/s.

remains nearly the same as L increases for all the specimens except that in pure Ti. The gradual decrease or constant value of μ with L indicates that wear in the laser-alloyed sample is predominantly abrasive in nature [23]. In this regard, the extent and rate of wear are minimum in Ti(Si) followed by that in Ti(Si + Al) and Ti(Al) (cf. Fig. 7). In pure Ti, the increase in μ with L at the initial stage may be attributed to severe adhesive wear, particularly at higher L. Subsequently, μ decreases with an increase in L at $L > 30$ N due to a possible change over from the adhesive to abrasive wear with three-body wear contributing in higher amount than the earlier two-body wear stage [23]. At still higher L (> 40 N), the anomalous change in μ with L in pure Ti is absent (Fig. 9(b)). Furthermore, μ decreases as L increases in all the cases. Perhaps, the wear in these cases is mostly abrasive in nature. It may be pointed out that n_w is low in Fig. 9(b), signifying a very low friction event at the initial stage of wear.

Fig. 10(a)–(d) show the typical microstructures of the worn-out surfaces after $n_w = 1000$ at $L = 40$ N. Under the present condition of wear, pure Ti suffers extensive amount of adhesive wear and localized deformation responsible for the formation and propagation of micro-cracks (Fig. 10(a)). Perhaps, the accumulated debris may offer partial lubrication during the later stage of wear test. Fig. 10(b) reveals that no significant amount of adhesive or abrasive wear has taken place in Ti(Si). In fact, the accumulated worn-out debris may induce a three-body wear-related low friction event at some stage of wear test. This microstructural evidence substantiates the earlier reported kinetic data of wear that the latter is minimum in Ti(Si) than in any other laser-alloyed samples (Figs. 6–9). In comparison, Ti(Al) suffers an extensive amount of both abrasive and adhesive wear (Fig. 10(c)). A close observation reveals that adhesive wear is associated with micro-cracks in this sample. However, smaller crack dimension and absence of substantial amount of accumulated debris suggest that Ti(Al) possesses a better resistance to wear than that in pure Ti. The relative improvement in wear resistance in Ti(Al) than that in pure Ti may be attributed to the solid solution hardening offered by the dissolved Al in the AZ of Ti(Al). Fig. 10(d) shows that Ti(Si + Al) undergoes wear mostly by abrasive mechanism. The large volume fraction of worn-out debris is likely to develop a three-body wear condition and partial lubrication to reduce μ after a certain stage of wear. It appears that Ti(Si) and Ti(Si + Al) suffer relatively smaller amounts of wear due to a hyper-eutectic

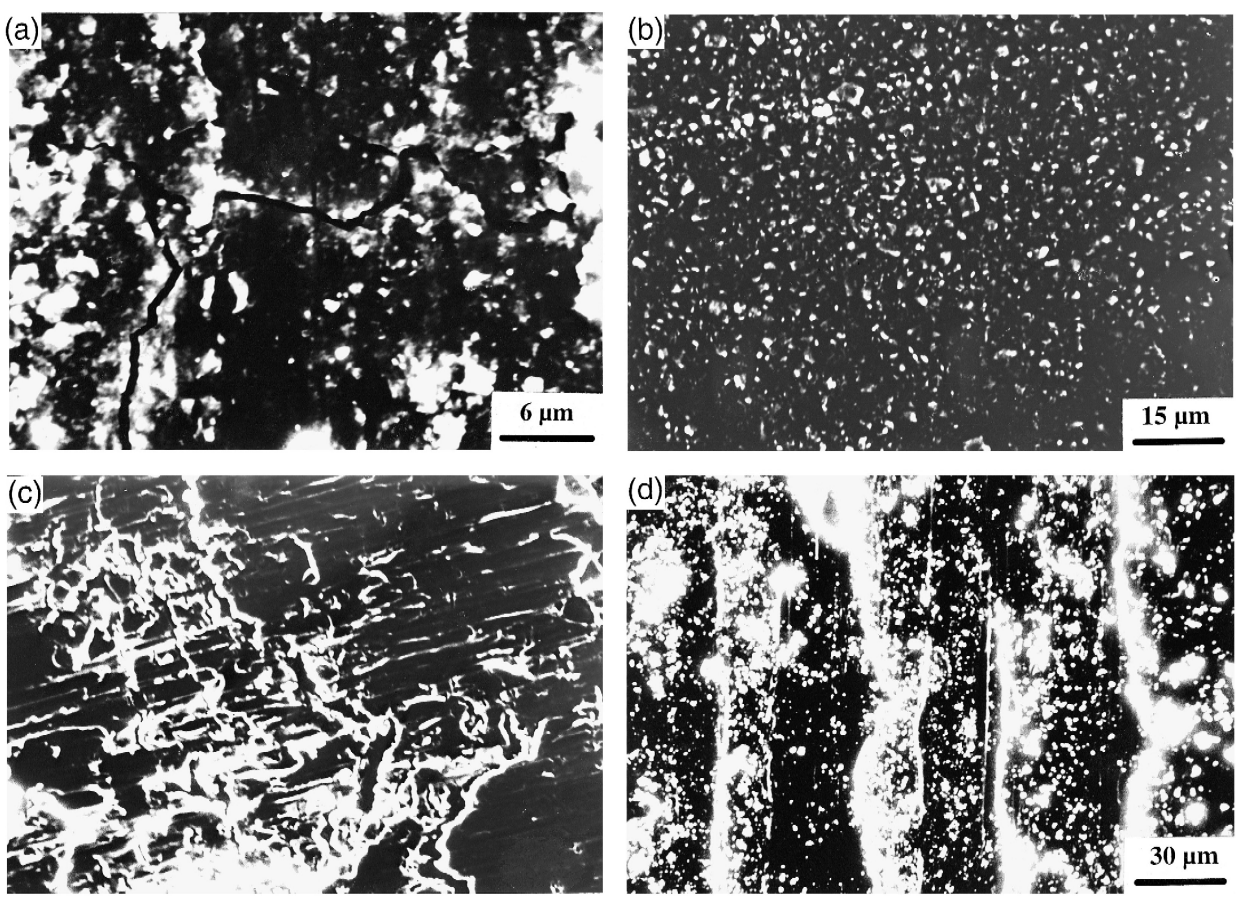

Fig. 10. Microstructure of the worn out surfaces of (a) pure Ti and laser-alloyed Ti with (b) Si, (c) Al, and (d) Si + Al. LSA was carried out with $P = 4$ kW, $v = 300$ mm/min and $F_p = 17$ mg/s.

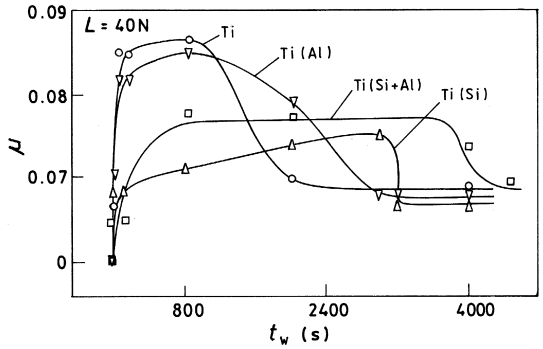

Fig. 11. Variation of μ of pure Ti and laser-alloyed Ti with Si, Al and Si + Al as a function of t_w ($L = 40$ N). LSA was carried out with $P = 4$ kW, $v = 300$ mm/min and $F_p = 17$ mg/s.

two phase microstructure of the concerned AZs (Fig. 2(b) and (d)) than that in pure Ti and Ti(Al) both having essentially a single phase microstructure (Fig. 2(a) and (c)). However, a close comparison between Fig. 10(b) and (d) reveals that both the extent and rate of wear are smaller in Ti(Si) than that in Ti(Si + Al). It is plausible that a relatively higher volume fraction of Ti_5Si_3 in Ti(Si) is associated with a better resistance to wear in the latter than that in Ti(Si + Al).

Finally, it is relevant to mention that EDS analysis of the wear debris does not reveal any significant contamination of Fe or Cr from the ball to the specimen. Furthermore, XRD analysis of these debris could not be undertaken due to the low volume of the later produced in the present wear studies.

3.7. Mechanism of wear

Fig. 11 shows the variation of μ as a function of t_w during a real time wear test with $L = 40$ N. Following an initial surge due to interlocking and smoothening of asperity to increase the real area of contact, a steady-state wear initiates in all the samples nearly at the same instant of time. The extent of wear is minimum in Ti(Si) and maximum in pure Ti. The wear behavior is identical in Ti and Ti(Al) on one hand, and Ti(Si) and Ti(Si + Al) on the other hand. In the former category, the steady-state wear is followed by a gradual decrease in the μ value with an increase in t_w. This decrease is more gradual and suspended in Ti(Al), perhaps due to solid solution hardening in the latter. On the other hand, wear in Ti(Si) and Ti(Si + Al) undergoes a low friction event following a sharp or gradual change over from the steady state, respectively. This low friction event may arise due to partial lubrication offered by the three-body wear condition involving the worn-out debris or due to frictional heating effects reducing μ. It is anticipated that the softer phase in the two phase eutectic aggregate in Ti(Si) or Ti(Si + Al) facilitates accumulation of debris at the initial stage, which subsequently acts as loose solid lubricant in between the indenter and high silicide-rich surface during the low friction steady-state event. It is interesting to note that the

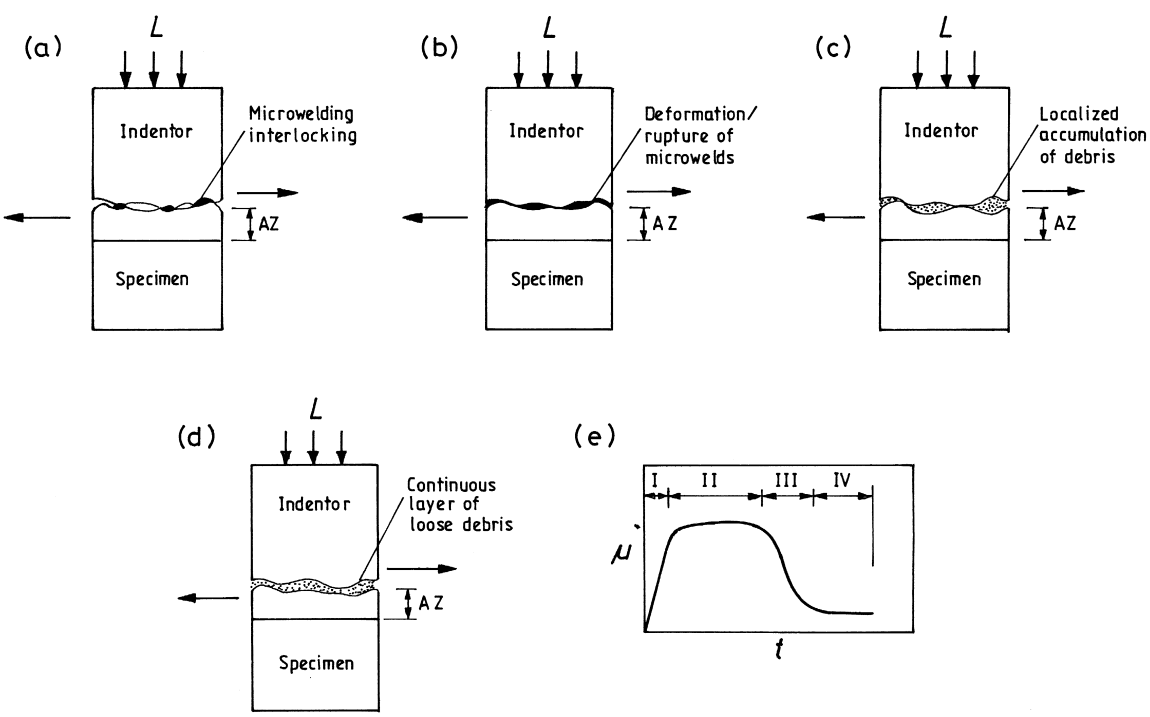

Fig. 12. Schematic illustration of the mechanism of wear in laser-alloyed samples: (a) micro-welding/interlocking phenomenon (stage I), (b) steady-state wear (stage II), (c) low friction or interface wearing event (stage III), (d) three-body wear condition (stage IV), and (e) schematic variation of μ with t showing the abovementioned four stages of wear.

μ values for all the samples tend to converge within a narrow range in the final stage (Fig. 11). This may be attributed to a possible three-body wear condition offered by the loose debris at the final stage.

To summarize, Fig. 12(a)–(f) schematically illustrate the general wear behavior of laser-alloyed samples investigated in this study.

Stage I Micro-welding/interlocking phenomenon (sudden rise in μ). It causes an increase in μ because of the alternate sequence of interlocking of surface asperity and micro-welding of the contact surface, leading to an increase in total area of frictional contact and frictional coefficient (Fig. 12(a)).

Stage II Steady-state wear (constant μ). During this stage, wear starts due to adhesion or abrasion depending on the nature of the contact surface and surface contour while μ remains almost constant or slightly increases if the adhesive bonding between the interacting surfaces is high (Fig. 12(b)).

Stage III Low friction or interface wearing event (gradual decreases in μ). During this stage the contact surfaces are set free due to detachment of worn-out debris as a result of which the μ decreases (Fig. 12(c)).

Stage IV Three-body steady-state phenomenon (constant μ). Once the worn-out debris get detached and occupy the space in between the contact surface, the system converts from a two-body to three-body wear condition during which μ remains constant as the loose powder particles tend to act as lubricants and reduce wear (Fig. 12(d)).

The above mentioned stages are schematically summarized in terms of variation of μ with t in Fig. 12(e). It may be noted that the precise range and dominance of each stage will primarily depend on the microstructure/composition and contour of the surfaces in contact under a given condition of wear.

4. Summary and conclusions

The present study shows that LSA is a potential route of enhancing wear resistance of pure Ti. The important conclusions emerging out of this study are the following.

(1) LSA of pure Ti with Si, Al and Si + Al increases the microhardness of the AZ by two to four times. While a two-phase hyper-eutectic microstructure is responsible for higher hardness in Ti(Si) and Ti(Si + Al), the similar enhancement in Ti(Al) is due to solid solution hardening in a single-phase microstructure.

(2) LSA significantly improves the wear resistance of laser surface-alloyed Ti subjected to wear testing with a hardened steel ball. The improvement is most effective in Ti(Si) followed by that in Ti(Si + Al) and Ti(Al) in decreasing order of wear resistance.

(3) LSA markedly reduces the coefficient of friction measured by quantitative wear testing. Here again, the reduction is most significant in Ti(Si) followed by that in Ti(Al) and Ti(Si + Al) in order of increasing coefficient of friction.

(4) The mechanism of wear has been studied by a detailed kinetic and microstructural investigation. Accordingly, the wear behavior under constant load has been divided into four stages, namely, micro-welding/interlocking phenomenon (stage I), steady-state wear comprising deformation/rupture of micro-welds (stage II), low friction or interface wearing event (stage III) and three-body wear condition (stage IV).

Acknowledgements

Dr. Dutta Majumdar expresses her gratitude to DAAD, Bonn for financial support during her stay in Germany. Similarly, partial financial support from the Council of Scientific and Industrial Research, New Delhi (Grant no. 22-0253-96) to Prof. Manna is gratefully acknowledged.

References

[1] M.J. Donachie Jr. (Ed.), Titanium and Titanium Alloys, ASM, Metals Park, OH, 1982, p. 3.
[2] S. Yerramareddy, S. Bahadur, Wear 142 (1992) 253–263.
[3] P.D. Miller, J.W. Holladay, Wear 2 (1958–1959) 133–140.
[4] W. Beck, J.F. Danovich, Wear 14 (1969) 15–32.
[5] A. Molinary, G. Straffelini, B. Tesi, T. Bacci, G. Pradelli, Wear 203/204 (1997) 447–454.
[6] T. Bell, H.W. Bergmann, J. Lanagan, P.H. Morton, A.M. Staines, Surf. Eng. 2 (1986) 133–143.
[7] J. Majumdar, J. Singh, in: C.W. Draper, P. Mazzoldi (Eds.), Laser Surface Treatments of Metals, Martinus Nijhoff, Dordrecht, 1986, pp. 297–308.
[8] H.W. Bergmann, in: C.W. Draper, P. Mazzoldi (Eds.), Laser Surface Treatments of Metals, Martinus Nijhoff, Dordrecht, 1986, pp. 351–368.
[9] C.H. Chen, M.K. Keshavan, C.J. Altstetter, J.M. Rigsbee, in: K. Mukherjee, J. Mazumdar (Eds.), Laser Processing of Materials, AIME, Warrendale, PA, 1985, pp. 183–197.
[10] J.D. Ayers, R.J. Schaefer, W.P. Robey, J. Met. 33 (1981) 19–23.
[11] P.A. Molian, in: T.S. Sudarshan (Ed.), Surface Modification Technologies — An Engineer's Guide, Marcel Dekker, New York, 1989, pp. 421–491.
[12] C.W. Draper, J.M. Poate, Int. Met. Rev. 30 (1985) 85–107.
[13] B.L. Mordike, in: R.W. Cahn, P. Haasen, E.J. Kramer (Eds.), Materials Science and Technology vol. 15 VCH, Weinheim, 1993, pp. 112–135.
[14] B.L. Mordike, in: C.W. Draper, P. Mazzoldi (Eds.), Laser Surface Treatments of Metals, Martinus Nijhoff, Dordrecht, 1986, pp. 389–412.
[15] J.D. Ayers, Wear 97 (1984) 249–266.
[16] S. Yerramareddy, S. Bahadur, Wear 157 (1992) 245–262.

[17] J. Dutta Majumdar, X. He, A. Weisheit, B.L. Mordike, I. Manna, Lasers Eng. 7 (1998) 89–102.
[18] J. Dutta Majumdar, A. Weisheit, B.L. Mordike, I. Manna, Mater. Sci. Eng., A 266 (1999) 123–134.
[19] J. Dutta Majumdar, A. Weisheit, B.L. Mordike, S.K. Roy and I. Manna, Oxid. Met. (Communicated).
[20] J.L. Murray, Phase Diagram of Binary Titanium Alloys, ASM, Metals Park, OH, 1987, p. 289, 12–13.
[21] E.S. Bumps, H.D. Kessler, M. Hansen, J. Met. 4 (1952) 607–609.
[22] J.F. Archard, J. Appl. Phys. 24 (1953) 981–988.
[23] K.C. Ludema, ASM Handbook vol. 18 ASM, Metals Park, OH, 1992, p. 236.